Detection of the heme perturbations caused by the quaternary $R \rightarrow T$ transition in oxyhemoglobin trout IV by resonance Raman scattering

Reinhard Schweitzer-Stenner, Dörte Wedekind, and Wolfgang Dreybrodt
University of Bremen, Physics Department, 2800 Bremen 33, Federal Republic of Germany

ABSTRACT The depolarization ratio dispersion and the respective excitation profiles of two structural sensitive Raman lines of oxyhemoglobin-trout IV (1,375 and 1,638 cm^{-1}) have been measured at pH-values between 6.5 and 8.5. They were analyzed by employing a fifth order time dependent perturbation theory to calculate the polarizability tensor. This provides information about the pH-dependence of parameters reflecting symmetry classified distortions of the prosthetic heme groups. In order to correlate these distortions with functional properties of the molecule the following protocol has been employed: (*a*) a titration model was formulated relating each conformation of the molecule to a distinct set of distortion parameters the incoherent superposition of which provides the respective distortion parameter obtained from our Raman data. (*b*) The thermodynamic constants determining the equilibrium between these molecular conformations (i.e., the quaternary *T* and *R*-states, the low affinity *t* and the high affinity *r*-states of the distinct subunits, the pK-values of the Root- and Bohr groups) were obtained from a set of O_2-binding curves that were analyzed in terms of an allosteric model suggested by Herzfeld and Stanley 1974. *J. Mol. Biol.* 82:231. The application of this procedure yields excellent reproduction of the pH-dependent effective distortion parameters of both Raman lines investigated. Thus established correlation between hemoglobin function (O_2-binding) and structure (asymmetric perturbation of the hemegroup) provides some interesting insights into the molecular basis of the allosteric Root effect.

INTRODUCTION

In the preceding paper (Schweitzer-Stenner and Dreybrodt, 1989) we have shown that the oxygen binding curves of hemoglobin trout IV (Hb trout IV) can be interpreted in terms of an $R \rightarrow T$ transition of the fully oxygenated molecule when approaching the acid pH-region (below pH = 7.0). This conformational change causes a significant decrease of the Hill coefficient which becomes smaller than one below pH = 6.5 (negative cooperativity). The subject of this paper concerns structural changes of the prosthetic group caused by the pH-induced $R \rightarrow T$ transition. It is well known from crystallographic studies of Perutz (1970*a*, *b*), Baldwin and Choita (1979), and Shaanan (1983), that binding of a ligand to the central iron atom of the prosthetic group effects significant changes of the tertiary structure of the respective subunit which causes a destabilization of intersubunit noncovalent contacts determining the quarternary *T*-state (*H*-bonds, saltbridges, cf. Ackers, 1980). This destabilization effect is amplified by subsequent ligand binding to other subunits. Hence in human hemoglobin the quarternary structure switches into a more relaxed state (*r*-state) upon ligation to three of the four subunits.

In order to understand the relationship between ligand affinity and the structure of the prosthetic group, numerous experiments have been dedicated to the investigation of the first step of this stereochemical cascade. It has been found that this process is associated with (*a*) the change of the Fe^{2+} spin state from high to low spin (Hoard, 1986; Perutz, 1970), (*b*) a core size expansion of the porphyrin (Ondrias et al., 1982), (*c*) a decrease of the electron density at the heme core (Shelnutt et al., 1979), and (*d*) the change of the force constant of the Fe^{2+}-His (F9) bond (Nagai et al., 1980; Ondrias et al., 1982). Furthermore Warshel and Weiss (1982) showed that the electrostatic potential of the porphyrin is drastically affected by the ligation process.

Despite these findings a lot of questions remain unsolved. It could not be clarified whether the free energy required for the allosteric $T \rightarrow R$ transition is stored in the heme apoprotein contacts (for instance the Fe^{2+}-His(F9) bond, cf. Nagai et al., 1980), in the intersubunit saltbridges (Ackers, 1980), or whether it is equally distributed over the entire protein (Hopfield, 1972; Agmon and Hopfield, 1983; Cobau et al., 1985). Furthermore, it is difficult to discriminate between the structural changes induced by the ligand binding and those which are due to $t \rightarrow r$ transitions of the subunits (cf. Rousseau et al., 1984; Friedman et al., 1983). Finally it has not yet been clarified which type of heme apoprotein interactions (i.e., histidine-heme, ligand-protein, protein-porphyrin side chains) mainly determines the ligand affinity.

Address all correspondence to Dr. Dreybrodt.

As we have shown in a former paper (Schweitzer-Stenner et al., 1984), resonance Raman scattering can be applied in order to detect distortions of the prosthetic heme group, which are due to different types of heme-protein interactions. This has been achieved by measuring the depolarization ratio dispersion (DPR) and the corresponding excitation profiles (EPs) of structural sensitive Raman lines. By a subsequent thorough analysis in terms of a fifth-order time dependent perturbation theory (Schweitzer-Stenner and Dreybrodt, 1985), this procedure provides distortion parameters which are linearly related to the amplitude of symmetry classified normal distortions $\delta Q^{\Gamma'}$ of the prosthetic group ($\Gamma' = A_{1g}$, B_{2g}, and A_{2g} representations in D_{4h}-symmetry).

The applicability of this method has recently been demonstrated by Schweitzer-Stenner et al. (1986) and Brunzel et al. (1986). They measured the pH-dependence of the DPR-dispersion of two prominent oxyHb-Raman-lines (1,375 and 1,638 cm^{-1}) at low Cl^--concentrations. The analysis of the data yielded a pH-dependence of the heme perturbation explained in terms of the following model: protonation processes of distinct amino acid side groups of the protein affect the conformation of the respective local environment. The thus-provided conformational changes are transduced to the porphyrin groups resulting in distortions which is specific to each titration state of the molecule. The measured Raman intensities are resulting from incoherent superposition of these distinct kinds of porphyrin molecules. The pH-dependence of the distortion parameters obtained from the analysis of the Raman experiments thus reflects the variation of the occupation numbers of the distinct titrable groups upon changing the pH-value of the solution.

Applying this model to oxyHb A, three titrable groups with pK = 5.8, 6.6, and 7.8 were obtained. In order to test the validity of the results, the same titration model has been directed to experimental data reflecting the pH-dependence of the optical absorption (Brunzel et al., 1986) and the fourth Adair constant (deYoung et al., 1976; Kwiatkowski and Noble, 1982; Schweitzer-Stenner et al., 1986). Excellent agreement in terms of the obtained pK-values has been achieved. This provides evidence that both, the pH-dependence of the heme-structure, detected by resonance Raman and absorption experiments and the respective variation of the fourth Adair constant, have one common reason.

In order to establish the correlation between ligand binding and heme-apoprotein interaction in hemoglobin trout IV we have applied this method of Raman investigation by adopting the following protocol. First we measured the depolarization ratio dispersion (DPD) and the corresponding EPs of the 1,375 cm^{-1} and the 1,638 cm^{-1}-fundamentals at different pH-values between 6.5 and 8.5. Second we extracted the pH-dependence of the heme distortions from these experimental data. Finally we employed a titration model considering the heme perturbations that are induced by structural changes of the protein due to the protonation of amino acid side chains influencing both, the tertiary states of the distinct subunits, and the equilibrium between the quarternary T and R states, respectively. The equilibrium constants of these protonation processes have been calculated by applying the allosteric model of Herzfeld and Stanley (1974) to oxygen binding curves reported by Brunori et al. (1978) described in detail in our preceding paper (Schweitzer-Stenner and Dreybrodt, 1989). Our results provide evidence, that the pH-induced $R \rightarrow T$ transition of the fully ligated molecule occuring below pH = 7.0 effects a change of the heme structure at the central (i.e., Fe^{2+}, pyrrole-nitrogens) and the peripheral parts (side chains, C_β-atoms) of the porphyrin.

Theoretical background

Raman theory

A detailed description of the theory applied to the Raman data has been given elsewhere (Schweitzer-Stenner and Dreybrodt, 1985). Here we present only the final equations employed in a fitting procedure from which the distortion parameters are determined.

Our theory is an extension of the PNSF-theory (Peticolas et al., 1970) which is based on Loudon's formalism (Loudon, 1973) into fifth order. Thus it considers the vibrational side bands of the B- and Q-bands by rationalizing the creation and subsequent annihilation of phonons giving rise to these bands. Symmetry perturbations of the heme due to asymmetric positions of the side chains and heme-apoprotein contacts are introduced into this formalism by expanding the vibronic coupling operator in the Hamiltonian with respect to these normal distortions $\delta' Q^{\Gamma'}$. This leads to the following expression for the vibronic coupling matrix elements:

$$C^{\Gamma}_{es} = \langle e | dH/dQ^{\Gamma}_R + d^2H/dQ^{\Gamma 2}_R dQ^{\Gamma',3} | s \rangle Q^R_{01} \delta Q^{\Gamma'}, \quad (1)$$

where $|e>, |s>$ denote the excited electronic states related to the Q- and B-absorption bands. The operators dH/dQ^{Γ}_R and $dH^2/dQ^{\Gamma}_R dQ^{\Gamma'}$ denote the vibronic coupling operator of the Raman mode in the ideal D_{4h} and its changes resulting from the perturbations of the heme moyety by normal distortions $\delta Q^{\Gamma'}$ respectively ($\Gamma' = A_{1g}$, B_{1g}, B_{2g}, A_{2g} in D_{4h}). $Q^R_{01} = \langle 0 | Q^R | 1 \rangle$ is the transition matrix element of the Raman vibration.

The matrix elements $c^{\Gamma}_{e,s}$ are used as free parameters in a fit to the experimental DPD-curves and EPs.

Formulation of the effective polarizibility tensor

So far the theory considers only one conformational type of Hb-molecules to be present. In reality, due to various protonation processes and conformational transitions, many different conformational states of the molecules with different polarizibility tensors are simultaneously present in the solution.

As has been shown elsewhere (Schweitzer-Stenner et al., 1984) each tensor element of the effective Raman tensor can be expressed by:

$$|\beta_{\mu\sigma}^{eff}| = \left\{ \sum_l X_l (\beta_{\mu\sigma})_l^2 \right\}^{1/2}, \qquad (2)$$

where X_l denotes the mole fraction of the lth-conformation, the corresponding Raman tensor is denoted by $(\beta_{\mu\sigma})_l$.

Some straightforward calculations lead to the following expression for the effective distortion parameters, which are the result of a fitting procedure

$$|c_{e,s}^{\Gamma}(\mathrm{pH})| = \left\{ \sum_l X_l (c_{e,s}^{\Gamma})_l^2 \right\}^{1/2}. \qquad (3)$$

$(c_{e,s}^{\Gamma})_l$ are the distortion parameters of the Raman fundamental related to the lth conformation.

MATERIALS AND METHODS

Preparation of hemoglobin trout IV

The blood for the preparation was obtained from commercially purchased trout. It was washed several times with 0.9% aqueous solution of NaCl containing EDTA to avoid coagulations and afterwards hemolized with distilled water. The obtained hemoglobin solution was then dialyzed against 0.1 M Tris-HCl buffer at pH = 9.1. After equilibation it was applied to a DEAE-Sephadex A50-column from Sigma Chemical Co., St. Louis, MO (dimension 40 × 2 cm). The pH-gradient elution was carried out using two containers, one with 0.1 M tris-HCl buffer at pH = 9.1 and the other with $KH_2P_2O_4$.

The different pH-values were adjusted dialyzing against 0.1 M tris-HCl-buffer (pH > 7.0) and 0.1 M bis-tris-HCl-buffer (pH < 7.0). The concentration of each sample was 1.0×10^{-3} M and monitored by measuring the optical absorbance with an HP-diode array spectrometer.

Experimental arrangement

The exciting radiation was obtained using an Argon ion laser from Spectra Physics, Darmstadt, FRG. The laser beam was polarized perpendicularly to the scattering plane and focussed by a cylindrical lens into a sample, which was situated in a pressure cell. In order to maintain full oxygenation of the molecule even at low pH-values partial oxygen pressures up to 30 atm could be maintained. To avoid photodissociation of the O_2-molecules low laser power was applied especially at low pH. The Raman radiation was measured in backscattering geometry. A polarization analyzer between sample and spectrometer enabled us to measure the intensity of the two components perpendicular (1) and parallel (2) to the scattering plane. A polarization scrambler was used to avoid different transmissions of the spectrometer for different polarizations. The Raman spectrum was analyzed with a Czerny-Turner double monochromator (Spex, Munich, FRG) collected by a photocounting system (Ortec, Munich, FRG), digitized by a microcomputer, where it was stored for further analysis.

To calculate the correct height of the Raman lines a program was employed to subtract fluorescence background and to decompose complex spectra into distinct Lorentz lines of defined width and height. The thus obtained relative intensities were corrected for the frequency dependence, the transmission of the spectrometer (el Naggar et al., 1985) and the power of the incident laser light.

As has been shown in earlier papers (el Naggar et al., 1985) corrections due to absorption and imaging errors are not necessary.

RESULTS

Fig. 1, *a* and *b* exhibit the DPD-curves of the 1,375 cm^{-1} fundamental (A_{1g} in D_{4h}) and the corresponding excitation profiles ($E = E_{\parallel} + E_{\perp}$) covering the preresonant region between the Soret- and the Q_v-band (22.000 cm^{-1} and 18.500 cm^{-1}) for various pH. Each DPD-curve

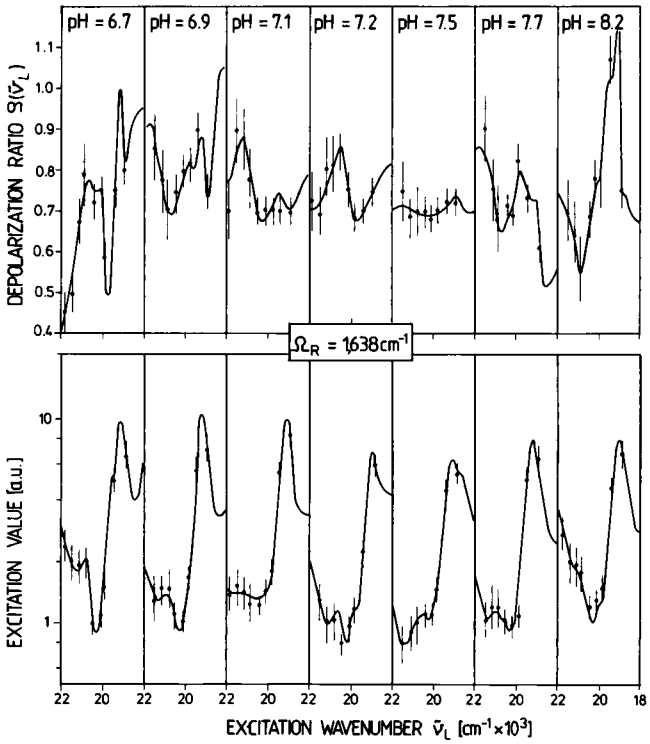

FIGURE 1 (*a*) DPR-dispersion curves of the 1,375 cm^{-1} line of oxyHb-trout IV at different pH-values. (*b*) Excitation profiles of the 1,375 cm^{-1} line of oxyHb-trout IV at different pH-values. The full lines result from the fitting procedure.

displays two significant maxima, the position of which changes with the pH-value. The smaller one is positioned between 21.500 and 20.500 cm^{-1}. The large maximum lies between 20.000 and 19.00 cm^{-1}. As one can read from Fig. 1 *b*, these maxima correspond to minima of the respective EP: the sharp and large maximum is situated between the Q_{01}/Q_{10} and the Q_{11}-resonance position. $Q_{\upsilon_R\upsilon_\mu}(\upsilon_R,\upsilon_\mu = 0, 1)$ relates to the energy $E_Q + \upsilon_R\Omega_R + \upsilon_\mu\Omega_\mu$, where Ω_R,Ω_μ denote the frequencies of the Raman fundamental and the effective phonon respectively (cf., Schweitzer-Stenner and Dreybrodt, 1985).

The DPD-curves and the EPs of the second fundamental investigated (i.e., 1,638 cm^{-1}, B_{1g} in D_{4h}) are depicted in Fig. 2, *a* and *b*. The DPD is very pronounced in the alkaline and the acid region (pH < 7.0 and pH > 7.5), exhibiting a similar maximum/minimum structure as the DPD-curves of the A_{1g}-fundamental. In the physiological region, however, the DPR-variation is comparatively small. This can be correlated with two observations obtained from the excitation profiles. In the alkaline and the acid region the contributions due to Q_{10}/Q_{01} and Soret resonance processes increase significantly, thus changing drastically the shape of the minimum at 20.300 cm^{-1}, positioned between the Q_{01}/Q_{10} and Q_{11}-resonances.

The full lines in Figs. 1–2 result from the application of our fitting procedure. Convincing agreements with the experimental data were established. These fits provide the values of the distortion parameters, c_{es}^{Γ} (pH) which are exhibited in dependence on the pH-value in Fig. 3 (1,375 cm^{-1}) and Fig. 4 (1,638 cm^{-1}). (It should be noticed that all parameter values are expressed in units of the respective c_{es}^{Γ} (pH = 6.6)-values). As one reads from these representations, the protonation of titrable amino acid residues affect both modes in a quite different manner: the c_{es}^{Γ}-values of the 1,375 cm^{-1}-fundamental are minimal at physiological values, but show a significant and sharp increase upon approaching the acid region. The distortion parameters of the 1,638 cm^{-1}, fundamental, however, show a maximum in the physiological region and decrease with acid and alkaline pH-values. The statistical errors of the c_{es}^{Γ}-values have been estimated to 15% in accordance with the variations obtained for oxyHb-BME (Wedekind et al., 1985). A detailed analysis of the pH-dependence of the distortion parameters is given in the next section.

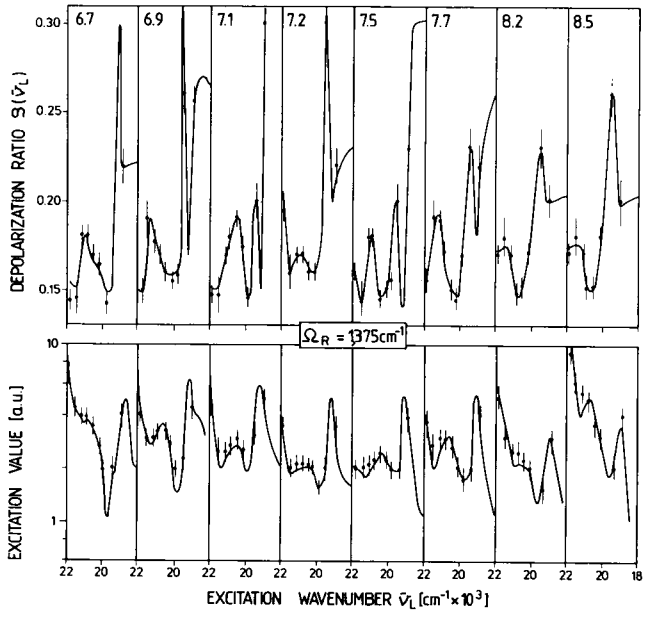

FIGURE 2 (*a*) DPR-dispersion curves of the 1,638 cm^{-1} line of oxyHb trout IV at different pH-values. (*b*) Excitation profiles of the 1,638 cm^{-1} line of oxyHb-trout IV at different pH-values. The full lines result from the fitting procedure.

DISCUSSION

PH dependence of the distortion parameters

In order to rationalize the pH-dependence of the effective distortion parameters c_{es}^{Γ} (pH) we consider the results of the analysis of the O_2-binding curves reported in the preceding paper in the following way: first we calculate the mole fraction X_1 of each conformation 1 by employing the equation:

$$X_1 = \exp\left\{\sum_j [G_1(\tau_j, q, \mathrm{pH})/RT]\right\}/Z, \qquad (4)$$

where Z denotes the grand partition sum and G_1

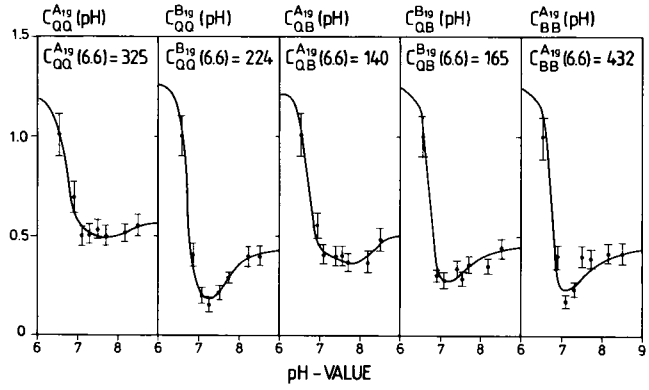

FIGURE 3 c_{es}^{Γ}(pH)-diagrams of the 1,375 cm^{-1}-fundamental of oxyHb-trout IV. The full lines result from the application of the tritration model.

(τ_j, q, pH) the Gibbs-free energy of the considered conformation 1. Both are expressed in terms of the following thermodynamical constants: (*a*) the equilibrium constants of the quarternary $T \rightarrow R$ transition and the tertiary $t \rightarrow r$ transitions of the different subunits, (*b*) the pK_t and the pK_r-values of the teritary effectors (Bohr groups), and (*c*) the pK_T and pK_R-values of the quarternary effectors (Root-groups). Each of these parameters has been obtained from the fit to experimental O_2-binding curves and are listed in the preceding paper (Schweitzer-Stenner and Dreybrodt, 1989).

Since in the context of this work (oxyHb) only the fully ligated molecules have to be considered, we calculate X_1 assuming the partial O_2-pressure to be very large. Fig. 5 displays the pH-dependent mole fractions of the predominant conformations. Only four states have to be taken explicitly into account:

$$S_1 = \{T, r_\alpha, r_\alpha, t_\beta, t_\beta\}[1, 1, 1, 1]$$
$$S_2 = \{R, r_\alpha, r_\alpha, r_\beta, r_\beta\}[1, 1, 0, 0]$$
$$S_3 = \{R, r_\alpha, r_\alpha, r_\beta, r_\beta\}[1, 0, 0, 0]$$
$$S_4 = \{R, r_\alpha, r_\alpha, r_\beta, r_\beta\}[0, 0, 0, 0].$$

$\{q, \tau_1, \tau_2, \tau_3, \tau_4\}$ $[i_{\alpha 1}, j_{\alpha 2}, k_{\beta 1}\, m_{\beta 2}]$ is related to the quarternary state q, the tertiary states τ_j of the jth subunit and the occupation numbers $i_{\alpha 1}$, $j_{\alpha 2}$, $k_{\beta 1}$, $m_{\beta 2}$ ($i_{\alpha 1}, j_{\alpha 2}, k_{\beta 1}$, $m_{\beta 2} = 0, 1$) of four titrable groups which to influence directly the oxygen binding affinity (Bohr effect, cf. Schweitzer-Stenner and Dreybrodt, 1989). The respective pk-values of these groups are denoted by $pK_{\alpha 1}$, $pk_{\alpha 2}$, $pK_{\beta 1}$, and $pK_{\beta 2}$. Their values were obtained from the fit to experimental O_2-binding curves and are listed in Table 1. The residual conformations exhibit very small mole fractions. Adding up their contributions one obtains the quantity X_R. Its pH-dependence is depicted in Fig 4. for comparison.

Second we relate each conformational state of the hemoglobin molecule to a distinct set of distortion parameters c_{es}^{Γ} $[i_{\alpha 1}, j_{\alpha 2}, k_{\beta 1}, m_{\beta 2}]$. Thus the effective parameters c_{es}^{Γ} (pH) obtained from our Raman experiments can be written as:

$$|C_{es}(\mathrm{pH})| = \{X_1(c_{es}^{\Gamma}[1, 1, 1, 1])^2 + X_2(c_{es}^{\Gamma}[1, 1, 0, 0])^2 + X_3(c_{es}^{\Gamma}[1, 0, 0, 0])^2 + X_4(c_{es}^{\Gamma}[0, 0, 0, 0])^2 + X_R[c_{es}^{\Gamma}(R)]^2\}^{1/2}, \quad (5)$$

where c_{es}^{Γ} $[i_{\alpha 1}, j_{\alpha 2}, k_{\beta 1}, m_{\beta 2}]$ denote the specific distortion parameters of the lth conformation the titration state of which is determined by the occupation numbers of $i_{\alpha 1}, j_{\alpha 2}$, $k_{\beta 1}, m_{\beta 2}$ of the four titrable groups. The parameters $c_{es,R}^{\Gamma}$ is related to the entire contribution of the conformations exhibiting small occupation numbers.

The parameters $c_{es}^{\Gamma}[i_{\alpha 1}, j_{\alpha 2}, k_{\beta 1}, m_{\beta 1}]$ and $c_{es,R}^{\Gamma}$ are used as free parameters in a fit to the obtained c_{es}^{Γ}(pH)-diagrams, whereas the equilibrium constants of all transitions considered in our titration model are taken from our preceding paper.

The result of these fits are displayed by full lines in Figs. 3 and 5. Sufficient agreement with the Raman data is established.

Thus evidence is provided that the pH-dependence of effective distortion parameters obtained from the analysis of our Raman data are related to structural processes affecting the oxygen affinity of Hb-trout IV. Tables 2 and 3 list the calculated values of the distortion parameters c_{es}^{Γ} $[i_{\alpha 1}, j_{\alpha 2}, k_{\beta 1}, m_{\beta 2}]$. From these the following aspects of the relationship between the heme-apoprotein interactions, the $R \rightarrow T$ transition and the protonation of Bohr groups emerge: (*a*) Large variations of the distortion parameters are caused by both, the pH-induced $R \rightarrow T$ transition (i.e., $S_2 \rightarrow S_1$; cf. Tables 2 and 3) and the protonation of Bohr-groups (i.e., the transitions $S_4 \rightarrow S_3$, $S_3 \rightarrow S_2$; cf. Tables 2 and 3). They affect the two modes investigated

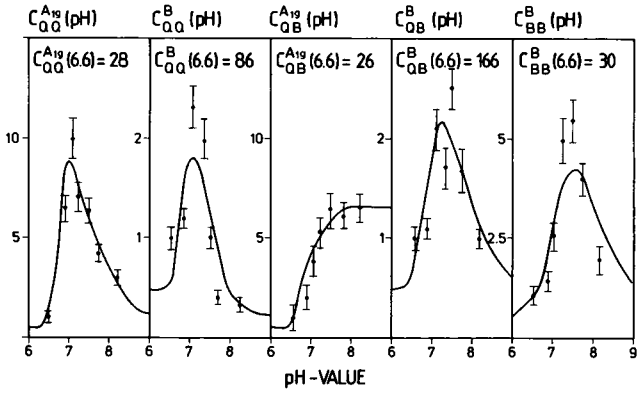

FIGURE 4 c_{es}^{Γ}(pH)-diagrams of the 1,638 cm^{-1}-fundamental of oxyHb-trout IV. The full lines result from the application of the titration model.

TABLE 1 PK values of the amino acid residues serving as tertiary effectors (Bohr groups) of the oxygen binding process

pk-assignment	Parameter values
$pK_{t_{\alpha 1}}$	8.5
$pK_{t_{\alpha 2}}$	8.5
$pK_{t_{\beta 1}}$	7.4
$pK_{t_{\beta 2}}$	7.5
$pK_{r_{\alpha 1}}$	7.0
$pK_{r_{\alpha 2}}$	7.6
$pK_{r_{\beta 1}}$	5.8
$pK_{r_{\beta 2}}$	5.9

Information taken from Schweitzer-Stenner and Dreybrodt, 1989.

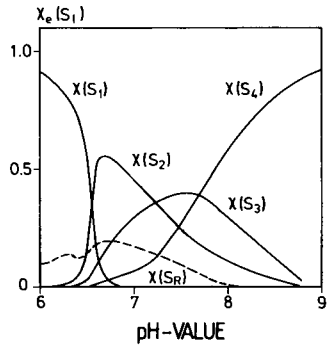

FIGURE 5 Mole fractions of the predominant conformations of oxyHb-trout IV in dependence on the pH-value.

TABLE 2 Distortion parameter values

Parameter	Parameter value	Configuration
	A_{1g}-contributions (1,375 cm^{-1})	
$c^{A1g}_{QQ}[0,0,0,0]$	0.58	$S_4 = \{R, r_{\alpha1}, r_{\alpha2}, r_{\beta1}, r_{\beta2}\}$ [0, 0, 0, 0]
$c^{A1g}_{QQ}[1,0,0,0]$	0.18	$S_3 = \{R, r_{\alpha1}, r_{\alpha2}, r_{\beta1}, r_{\beta2}\}$ [1, 0, 0, 0]
$c^{A1g}_{QQ}[1,1,0,0]$	0.77	$S_2 = \{R, r_{\alpha1}, r_{\alpha2}, r_{\beta1}, r_{\beta2}\}$ [1, 1, 0, 0]
$c^{A1g}_{QQ}[1,1,1,1]$	1.25	$S_1 = \{T, r_{\alpha1}, r_{\alpha2}, t_{\beta1}, t_{\beta2}\}$ [1, 1, 1, 1]
$c^{A1g}_{QQ,R}$	0.77	S_R
$c^{A1g}_{QB}[0,0,0,0]$	0.46	$S_4 = \{R, r_{\alpha1}, r_{\alpha2}, r_{\beta1}, r_{\beta2}\}$ [0, 0, 0, 0]
$c^{A1g}_{QB}[1,0,0,0]$	0.10	$S_3 = \{R, r_{\alpha1}, r_{\alpha2}, r_{\beta1}, r_{\beta2}\}$ [1, 0, 0, 0]
$c^{A1g}_{QB}[1,1,0,0]$	0.57	$S_2 = \{R, r_{\alpha1}, r_{\alpha2}, r_{\beta1}, r_{\beta2}\}$ [1, 1, 0, 0]
$c^{A1g}_{QB}[1,1,1,1]$	1.27	$S_1 = \{T, r_{\alpha1}, r_{\alpha2}, t_{\beta1}, t_{\beta2}\}$ [1, 1, 1, 1]
$c^{A1g}_{QB,R}$	0.57	S_R
$c^{A1g}_{BB}[0,0,0,0]$	0.44	$S_4 = \{R, r_{\alpha1}, r_{\alpha2}, r_{\beta1}, r_{\beta2}\}$ [0, 0, 0, 0]
$c^{A1g}_{BB}[1,0,0,0]$	0.21	$S_3 = \{R, r_{\alpha1}, r_{\alpha2}, r_{\beta1}, r_{\beta2}\}$ [1, 0, 0, 0]
$c^{A1g}_{BB}[1,1,0,0]$	0.57	$S_2 = \{R, r_{\alpha1}, r_{\alpha2}, r_{\beta1}, r_{\beta2}\}$ [1, 1, 0, 0]
$c^{A1g}_{BB}[1,1,1,1]$	1.30	$S_1 = \{T, r_{\alpha1}, r_{\alpha2}, t_{\beta1}, t_{\beta2}\}$ [1, 1, 1, 1]
$c^{A1g}_{BB,R}$	0.57	S_R
	B_{1g}	
$c^{B1g}_{QQ}[0,0,0,0]$	0.44	$S_4 = \{R, r_{\alpha1}, r_{\alpha2}, r_{\beta1}, r_{\beta2}\}$ [0, 0, 0, 0]
$c^{B1g}_{QQ}[1,0,0,0]$	0.10	$S_3 = \{R, r_{\alpha1}, r_{\alpha2}, r_{\beta1}, r_{\beta2}\}$ [1, 0, 0, 0]
$c^{B1g}_{QQ}[1,1,0,0]$	0.25	$S_2 = \{R, r_{\alpha1}, r_{\alpha2}, r_{\beta1}, r_{\beta2}\}$ [1, 1, 0, 0]
$c^{B1g}_{QQ}[1,1,1,1]$	1.30	$S_1 = \{T, r_{\alpha1}, r_{\alpha2}, t_{\beta1}, t_{\beta2}\}$ [1, 1, 1, 1]
$c^{B1g}_{QQ,R}$	0.25	S_R
$c^{B1g}_{QB}[0,0,0,0]$	0.45	$S_4 = \{R, r_{\alpha1}, r_{\alpha2}, r_{\beta1}, r_{\beta2}\}$ [0, 0, 0, 0]
$c^{B1g}_{QB}[1,0,0,0]$	0.42	$S_3 = \{R, r_{\alpha1}, r_{\alpha2}, r_{\beta1}, r_{\beta2}\}$ [1, 0, 0, 0]
$c^{B1g}_{QB}[1,1,0,0]$	0.20	$S_2 = \{R, r_{\alpha1}, r_{\alpha2}, r_{\beta1}, r_{\beta2}\}$ [1, 1, 0, 0]
$c^{B1g}_{QB}[1,1,1,1]$	1.29	$S_1 = \{T, r_{\alpha1}, r_{\alpha2}, t_{\beta1}, t_{\beta2}\}$ [1, 1, 1, 1]
$c^{B1g}_{QB,R}$	0.25	S_R

Distortion parameter values $c^{r\alpha}$ $[i, j, k, m]$ of the titration states resulting from the fit to the 1,375 cm^{-1} $c^{r\alpha}$ (pH)-diagrams (note that all parameters are expressed in terms of the respective $c^{r\alpha}$ (pH = 6.6)-values, which are displayed on the top of each diagram.

TABLE 3 Distortion parameter values

Parameter	Parameter value	Configuration
	B_{1g}-contributions (1,638 cm^{-1})	
$c^{A1g}_{QQ}[0,0,0,0]$	0.50	$S_4 = \{R, r_{\alpha1}, r_{\alpha2}, r_{\beta1}, r_{\beta2}\}$ [0, 0, 0, 0]
$c^{A1g}_{QQ}[1,0,0,0]$	1.50	$S_3 = \{R, r_{\alpha1}, r_{\alpha2}, r_{\beta1}, r_{\beta2}\}$ [1, 0, 0, 0]
$c^{A1g}_{QQ}[1,1,0,0]$	11.00	$S_2 = \{R, r_{\alpha1}, r_{\alpha2}, r_{\beta1}, r_{\beta2}\}$ [1, 1, 0, 0]
$c^{A1g}_{QQ}[1,1,1,1]$	0.50	$S_1 = \{T, r_{\alpha1}, r_{\alpha2}, t_{\beta1}, t_{\beta2}\}$ [1, 1, 1, 1]
$c^{A1g}_{QQ,R}$	1.00	S_R
$c^{A1g}_{QB}[0,0,0,0]$	7.00	$S_4 = \{R, r_{\alpha1}, r_{\alpha2}, r_{\beta1}, r_{\beta2}\}$ [0, 0, 0, 0]
$c^{A1g}_{QB}[1,0,0,0]$	5.50	$S_3 = \{R, r_{\alpha1}, r_{\alpha2}, r_{\beta1}, r_{\beta2}\}$ [1, 0, 0, 0]
$c^{A1g}_{QB}[1,1,0,0]$	1.50	$S_2 = \{R, r_{\alpha1}, r_{\alpha2}, r_{\beta1}, r_{\beta2}\}$ [1, 1, 0, 0]
$c^{A1g}_{QB}[1,1,1,1]$	0.50	$S_1 = \{T, r_{\alpha1}, r_{\alpha2}, t_{\beta1}, t_{\beta2}\}$ [1, 1, 1, 1]
$c^{A1g}_{QB,R}$	1.00	S_R
	B_{1g} and B_{2g}	
$c^{B}_{QQ}[0,0,0,0]$	0.50	$S_4 = \{R, r_{\alpha1}, r_{\alpha2}, r_{\beta1}, r_{\beta2}\}$ [0, 0, 0, 0]
$c^{B}_{QQ}[1,0,0,0]$	0.70	$S_3 = \{R, r_{\alpha1}, r_{\alpha2}, r_{\beta1}, r_{\beta2}\}$ [1, 0, 0, 0]
$c^{B}_{QQ}[1,1,0,0]$	2.26	$S_2 = \{R, r_{\alpha1}, r_{\alpha2}, r_{\beta1}, r_{\beta2}\}$ [1, 1, 0, 0]
$c^{B}_{QQ}[1,1,1,1]$	0.50	$S_1 = \{T, r_{\alpha1}, r_{\alpha2}, t_{\beta1}, t_{\beta2}\}$ [1, 1, 1, 1]
$c^{B}_{QQ,R}$	1.0	S_R
$c^{B}_{QB}[0,0,0,0]$	0.40	$S_4 = \{R, r_{\alpha1}, r_{\alpha2}, r_{\beta1}, r_{\beta2}\}$ [0, 0, 0, 0]
$c^{B}_{QB}[1,0,0,0]$	1.63	$S_3 = \{R, r_{\alpha1}, r_{\alpha2}, r_{\beta1}, r_{\beta2}\}$ [1, 0, 0, 0]
$c^{B}_{QB}[1,1,0,0]$	2.20	$S_2 = \{R, r_{\alpha1}, r_{\alpha2}, r_{\beta1}, r_{\beta2}\}$ [1, 1, 0, 0]
$c^{B}_{QB}[1,1,1,1]$	0.50	$S_1 = \{T, r_{\alpha1}, r_{\alpha2}, r_{\beta1}, r_{\beta2}\}$ [1, 1, 1, 1]
$c^{B}_{QB,R}$	0.50	S_R
$c^{B}_{BB}[0,0,0,0]$	0.50	$S_4 = \{R, r_{\alpha1}, r_{\alpha2}, r_{\beta1}, r_{\beta2}\}$ [0, 0, 0, 0]
$c^{B}_{BB}[1,0,0,0]$	3.40	$S_3 = \{R, r_{\alpha1}, r_{\alpha2}, r_{\beta1}, r_{\beta2}\}$ [1, 0, 0, 0]
$c^{B}_{BB}[1,1,0,0]$	1.50	$S_2 = \{R, r_{\alpha1}, r_{\alpha2}, r_{\beta1}, r_{\beta2}\}$ [1, 1, 0, 0]
$c^{B}_{BB}[1,1,1,1]$	0.50	$S_1 = \{T, r_{\alpha1}, r_{\alpha2}, t_{\beta1}, t_{\beta2}\}$ [1, 1, 1, 1]
$c^{B}_{BB,R}$	1.00	S_R

Distortion parameter values $c^{r\alpha}$ $[i, j, k, m]$ of the titration states resulting from the fit to the 1,638 cm^{-1} $c^{r\alpha}$ (pH)-diagrams (note that all parameters are expressed in terms of the respective $c^{r\alpha}$ (pH = 6.6)-values, which are displayed on the top of each diagram.

in a quite different manner: the c^{Γ}_{es} (pH)-values of the 1,375 cm^{-1}-mode increase strongly towards the acid and less pronounced towards the alkaline region whereas the respective parameters of the 1,638 cm^{-1}-fundamental display a maximum at physiological pH and decrease towards acid and alkaline pH. (*b*) The A_{1g}-contributions of the oxidation markerline (1,375 cm^{-1}) (reflecting A_{1g}-distortions) are affected by both, the $R \rightarrow T$ transition and the protonation of Bohr-groups. The corresponding B_{1g}-distortion parameters (reflecting B_{1g}-distortions), however, are mainly influenced by the $R \rightarrow T$ transition. This indicates that the allosteric transition provides an enhancement of asymmetric B_{1g} heme perturbations (lowering the symmetry of the porphyrin in contrast to the A_{1g}-distortions. (*c*) In the case of the spinmarker mode (1,638 cm^{-1}) both types of distortion parameters, i.e., c^{A1g}_{es} (now reflecting B_{1g}-distortions) and c^{B}_{es} (now reflecting A_{1g}

and A_{2g}-distortions) are influenced by the protonation of Bohr-groups as well as by the allosteric transition.

These findings indicate that different types of heme-apoprotein interactions influence the two Raman modes investigated. This effect can be explained by considering the normal vibrations of the υ_4 and the υ_{10}-mode of octaethylporphyrin that correspond to the 1,375 cm^{-1} and the 1,638 cm^{-1}-modes. Hence the following picture of heme-apoprotein interaction emerges from our Raman data.

His(F8)-heme interaction

The normal vibration of the υ_4 (oxidation marker) mode exhibits large vibrational amplitudes of the pyrrole nitrogens due to C_β-N stretching vibrations. For the υ_{10}-mode, however, these amplitudes are negligible (Abe et al., 1978). Therefore all perturbations affecting mainly these nitrogen atoms are exclusively monitored by the distortion parameters of the oxidationmarker line (υ_4). Thus asymmetric B_{1g}-perturbations induced by the $R \rightarrow T$ transition that has been established for this fundamental are due to distortions of the heme core. This type of perturbations results most probably from an increase of the repulsive interaction between the pyrrole nitrogens and the proximal histidine, which in the T-state is in a more tilt position with respect to the heme plane (Warshel, 1977; Gellin and Karplus, 1977).

This interpretation is in accordance with the correlation between the frequencies of the Fe^{2+}-N-His(F8)-stretching mode and the υ_4-mode obtained by Ondrias et al. (1982) over a wide variety of deoxyhemoglobins.

In the light of these considerations two questions have to be answered: first one has to elaborate whether the structural conformation of the central heme-apoprotein interface in the quarternary T-state (i.e., a more tilt position of the proximal imidazole which effects an asymmetric perturbation of the heme core via repulsive forces between pyrrole nitrogens and the imidazole) is related to the ligand affinity. Second one has to consider the structural relationship between the quarternary $R \rightarrow T$ transition and the experimentally observed conformational change of the tertiary structure.

We address these questions by the following considerations. As we have mentioned above, the predominant T-state conformation (i.e., $S_1 = \{T, r_\alpha, r_\alpha, t_\beta, t_\beta\}$ [1, 1, 1, 1]) contains only two subunits existing in the low affinity t-state whereas the other two subunits remain in the high affinity r-state. In our preceding paper (Schweitzer-Stenner and Dreybrodt, 1988) we have assigned the two t-subunits to the β-chains, because experimental evidence is provided that the conformational changes in the β-subunits are mainly responsible for the Root-effect (Perutz and Brunori, 1982; Condo et al., 1987). Therefore only conformational changes occurring in the β-subunits can be assigned to variations of the oxygen affinity.

In order to clarify whether the obtained B_{1g}-distortions of the pyrrole nitrogens can be assigned mainly to the porphyrins of the β-subunits we compare the results of this study with the findings that emerged from an earlier Raman study on oxyHb. Schweitzer-Stenner et al. (1986) have measured the pH-dependence of the DPR-dispersion of the υ_4 and the υ_{10}-modes of oxyHb A at low Cl^--concentrations. The analysis of the experimental data yielded that the distortion parameters c_{es}^{Γ} (pH) increase with decreasing pH. Even though the effect is less pronounced than that obtained for oxyHb-trout IV (especially for the υ_4-mode), it has a functional meaning that could be demonstrated by employing the same titration model in order to explain the pH-dependence of both, the heme perturbations and the fourth Adair constant (de Young et al. [1976]; Kwiatkowski and Noble [1982]). Hence a correlation between the increase of the heme distortion and the decrease of the equilibrium constant of the fourth binding step could be established. The structural nature of this correlation emerged from the comparison of kinetic experiments on oxyHB-A and on oxyHb modified in its β-subunit (i.e., des[His(HC3)β]-Hb, and des[His(HC3)β] des[Tyr(HC2)β]-Hb). In oxyHb A the protonation of histidine residues (pK = 6.6, perhaps His[HC3]β) influences the equilibrium between two conformations of the Tyr(HC2)β-ring, which has been related by Shaanan, 1983 to an oxy-like r and a deoxy-like t tertiary conformation. Hence we concluded that the obtained pH-dependent variation of the heme distortions of oxyHb A occur mainly in the β-subunits. This assignment is in accordance with the fact that the β-chain modified oxyHb-BME does not exhibit any significant pH-dependence of its heme structure (Wedekind et al., 1985, 1986). In this molecule cooperativity and Bohr-effect are absent because of a covalent crosslinking between His(FG4)β and Cys(F9)β by bis(N-maleimidomethyl) ether (Moffat, 1971), which imposes molecular strain on the FG-helix of the β-subunit. This most probably blocks the transduction of the conformational changes of the Tyr(HC2)β-ring to the chromophore and vice versa.

It is reasonable to assume that the molecular basis of the tertiary structure variations which give rise to the asymmetric distortions of the heme, are similar for oxyHb A and oxyHb-trout IV, whereas the interaction between quarternary and tertiary transitions is quite different. This can be rationalized in terms of stereochemical investigations reported by Perutz and Brunori (1982). In human Hb the F9-position of the β-subunits is occupied

by cystein. In Hb-trout this is substituted by serine. The OH^--group of Ser(F9)β can donate an H-bond to the carboxyl group of the COOH histidine His(HC3)β keeping it in a more internal position. This enables its imidazole to donate an H-bond to Glu(FG1)β upon protonation in both, the ligated and the unligated state of the β-subunit. This network of H-bonds stabilizes the COOH saltbridges and the $\alpha\beta$-interface thus providing a predominance of the *T*-state at acid pH. In the quarternary *T*-state the Tyr(HC3)β occupies exclusively the deoxylike position (Shaanan, 1983). In human Hb A, however, the COOH histidine donates an H-bond to Asp(FG4) upon protonation of its imidazole residue. It has not yet been clarified, whether this H-bond is ruptured in oxyHB A at low Cl^--concentrations (cf. Perutz, 1970; Russu et al., 1982; Kilmartin et al., 1980, Perutz et al., 1984, 1985; Wedekind et al., 1985). In each case a shift of the [T]/[R]-ratio of the fully oxgenated molecule is not achieved at acid pH. Therefore the protonation of His(HC3)β is not effective in shifting the equilibrium between the oxy and the deoxylike-position of Tyr(HC2)β. In other words, in oxyHb A the [t]/[r]-ratio of the β-subunits is smaller than that of oxyHB-trout IV at acid pH-values. This is reflected by less pronounced variations of the distortion parameters of the oxyHb A-υ_4-mode.

Hence, in light of these considerations, we conclude, that the increase of asymmetric perturbations of the heme core at acid pH as is monitored by the pH-dependence of the distortion parameters of the 1,375 cm^{-1}-fundamental are most probably due to tertiary transitions in the β-subunits. These cause a more tilt position of the proximal imidazole. This conformational change of the His(F9)β-heme interface is most probably responsible for the decrease of oxygen affinity as it is reflected by the $r \rightarrow t$ transition.

This conclusion is in excellent accordance with experimental data. The general shape of all c_{cs}^{Γ}(pH)-diagrams of the υ_4-mode is very similar to the pH-dependence of the average relaxation time of O_2-binding to Hb-trout IV as has been reported by Giardina et al. (1973).

It should be further mentioned that our interpretation corroborates a stereochemical model suggested by Friedman et al (1982, 1983) dealing with the relationship between $R \rightarrow T$ transitions and heme-apoprotein interaction. Due to their model the $R \rightarrow T$ transition of the ligated molecule causes a more strained $\alpha\beta$-interface which changes the position of the F-helix thus affecting a tilt of the proximal imidazole with respect to the hem plant (cf. also Baldwin and Choita, 1980). This increases the repulsive forces between the imidazole and the pyrrole nitrogens (cf. for carp Hb; Chance et al., 1986) thus inducing asymmetric perturbations into the heme core. Additionally Friedman et al. (1983) proposed a correlation among the energy of the imidazole-*N*(pyrrole) repulsion and the dissociation rate of ligand binding. In terms of our parameters, this means that the increase of the υ_4-distortion parameters is correlated with the enhancement of ligand dissociation.

Interaction between the heme side chains and the protein environment

As has been pointed out before, the υ_{10}-mode of the porphyrin molecule does not exhibit amplitudes of the nitrogen pyrroles. Due to Abe et al. (1978) its normal vibration can be described as a superposition of C_α and C_m-stretching modes and vibrations of the peripheral C_β-atoms, nearly parallel to C–C bonds between the C_β-atoms and the porphyrin side chains.

The vibronic perturbation monitored by the drastic dispersion of the DPR is most probably caused via the vinyl- and propionic side chains of the porphyrin. It is well known that the vinyl groups participate in the π-electron system of the porphyrin (Hsu, 1970). The extent depends on the orientation of the vinyl groups with respect to the heme plane, which is adjusted by the noncovalent van der Waals contacts between the vinyl groups and the protein environment. One of these contacts, a van der Waals bond between the vinyl group of pyrrole 3 and Val(FG5) was shown to be quite sensitive to quarternary transitions in human hemoglobin(Gellin and Karplus, 1977). Therefore it is reasonable to assume that this bond provides a pathway to transduce conformational changes of the protein to the peripheral part of the porphyrin. This is reflected by variations of the distortion parameters of the υ_{10}-mode.

Wedekind et al. (1985, 1986) provided experimental evidence that the protein-side chain interaction affecting the υ_{10}-mode does not influence the vibronic properties of the υ_4-mode significantly.

As one can read from Table 3 the quarternary $R \rightarrow T$ transition is correlated with a strong decrease of the υ_{10}-distortion parameter values. Attributing this finding to the interaction among Val(FG5) and the vinyl group of pyrrole 3 one concludes that the angle between the vinly group and the porphyrin increases upon $R \rightarrow T$ transition. This implies that Val(FG5) is pushed away from pyrrole 3.

This interpretation is consistent with the results of stereochemical investigations reported by Gellin and Karplus (1977). They found that for human hemoglobin the distance between Val(FG5) and pyrrole 3 increases upon oxygen binding ($\approx$1Å). Because the tertiary structure of

the low affinity state does not change significantly upon ligand binding (Baldwin and Choita, 1980), this conformational change can be attributed to the $R \rightarrow T$ transition.

Now the question arises whether this structural variation can be assigned to the respective $r \rightarrow t$ transition. In this case the effect would exclusively occur in the *b*-subunits. The obtained pH-dependent of the υ_{10}-mode, however, it is not in accordance with this prediction. As one can learn from Table 3, the protonation of the amino acid residues assigned to the α-subunits ($pK_{r\alpha 1} = 7.8$ and $pK_{r\alpha 2} = 7.4$) causes a significant increase of the vibronic perturbation, in contrast to what did emerge from the analysis of the 1,375 cm^{-1}-fundamental. The $R \rightarrow T$ transition counteracts this enhancement of the perturbations. Therefore we conclude that the respective variations of the tertiary conformation occur predominantly in the α-subunits, which has been found to remain in the *r*-state even if the entire molecule exists in the quarternary *T*-state.

It cannot be excluded that the $T \rightarrow R$ transition affects also the Val(FG5)β-vinyl interaction in the β-subunits, but this effect cannot be extracted from the data because of the overwhelming influence of the protonation occurring in the α-subunits.

An assignment of the obtained $pK_{r\alpha}$-values to distinct amino acid residues is actually not possible because no information is available about the contribution of the α-subunit to the alkaline Bohr effect in Hb trout IV.

We summarize our results as follows: (*a*) We have examined the DPR-dispersion of the oxidation-marker (1,375 cm^{-}) and the spinmarker (1,638 cm^{-1}) line of the oxyHb-trout IV Raman spectrum measured at different pH-values between 6.5 and 8.5. From this we obtain the pH-dependence of symmetry classified normal distortions. (*b*) The pH-dependent heme distortions are interpreted in terms of a titration model which relates each conformation of the molecule to a distinct set of distortion parameters. The thermodynamic constants determining the equilibrium between these molecular conformations (i.e., the quarternary *T* and *R*-states, the low affinity *t* and the high affinity *r*-states of the distinct subunits, the pK-values of the Root- and Bohr-groups) were obtained from a set of O_2-binding curves by a thorough analysis in terms of an allosteric model suggested by Herzfeld and Stanley (1972). (*c*) Thus the following correlations between structural and functional properties of oxyHb-trout IV could be established. The pH-dependent $R \rightarrow T$ transition effects a tilted position of the proximal imidazole of the β-subunit with respect to the heme plane. This conformational change enhances the repulsive forces between the imidazole carbon and the pyrrole nitrogens of the heme. These pertubations are monitored by the increase of the B_{1g}-type distortion parameters of the 1,375 cm^{-1}-fundamental towards acid pH-values.

The Val(FG)5-group of the α-subunits, which is in close contact with the vinyl side chain of pyrrole 3 is most probably pushed away from the heme upon the $R \rightarrow T$ transition because of the conformational changes of the $\alpha_1\beta_2/\alpha_2\beta_1$-interfaces.

We acknowledge gratefully that Professor Beyersmann (FB 2-Chemie) helped to implement the preparation of hemoglobin trout IV Reinhard Schweitzer-Stenner would like to thank Dr. Shaanan (Weitmann Institute) for helpful discussions concerning the stereochemistry of hemoglobin. Finally we thank Diplom-Physikar U. Bobinger who was involved in the preparation procedure and Mr. G. Ankele for technical assistance and for drawing the figures.

Received for publication 13 may 1988.

REFERENCES

Ackers, G. K. 1980. Energetics of subunit assembly and ligand binding in human hemoglobin. *Biophys. J.* 43:331–343.

Abe, M., T. Kitagawa, and Y. Kyogoku. 1978. Resonance Raman spectra in octaethylporphyrin-Ni(II) and mesodeuterated and ^{15}N-substituted derivatives. II. A normal coordinate analysis. *J. Chem. Phys.* 69:4526–4534.

Agmon, N., and J. J. Hopfield. 1983. CO-binding to heme proteins. *J. Chem. Phys.* 79:2042-2053.

Baldwin J. L., and C. Choita. 1979. Haemoglobin, the structural changes related to ligand binding and its allosteric mechanism. *J. Mol. Biol.* 129:175–200.

Brunori M., C. Coletta, B. Giardina, and J. Wyman. 1978. A macromolecular transducer as illustrated by trout-hemoglobin IV. *Proc. Natl. Acad. Sci. USA.* 75:4310-4312.

Brunzel U., W. Dreybrodt, and R. Schweitzer-Stenner. 1986. PH-dependent absorption in the B and Q bands of oxyhemoglobin and chemically modified oxyhemoglobin (BME) at low Cl^{-}-concentrations. *Biophys. J.* 49:1069–1076.

Condo, S. G., B. Giardina, A. Bellelli, and M. Brunori. 1987. *Xenopus laevis* Hemoglobin and its Hybrids with Hemoglobin A. *Biochemistry.* 26:6718–6722.

Chance, M. R., L. J. Packhurst, L. S. Powers, and B. Chance. 1986. Movement of Fe with respect to the heme plane in the R → T transition of carp hemoglobin. *J. Biol. Chem.* 261:5689–5692.

Cobau, W. G., J. D. LeGrange, and R. H. Austin. 1985. Kinetic differences at low temperatures between R- and T- state carbonmonoxide-carp hemoglobin. *Biophys. J.* 47:781–786.

Friedman, J. M., T. W. Scott, R. A. Stepnowski, M. Ikedo-Saito, and R. L. Cone. 1983. The Iron-proximal histidine linkage and protein control of oxygen binding in hemoglobin. *J. Biol. Chem.* 258:10564–10572.

Friedman, J. M., R. A. Stepnowski, M. Stavola, M. R. Ondrias, and R. L. Cone. 1982. Ligation and quarternary structure induced changes in the heme pocket of hemoglobin: a transient Raman study. *Biochemistry.* 1982:2022–2028.

Gellin B. R., and M. Karplus. 1977. Mechanism of tertiary structural change in hemoglobin. *Proc. Natl. Acad. Sci. USA.* 74:801–805.

Giardina, B., M. Brunori, I. Binatti, S. Giovenco, and E. Antonini. 1973. Studies on the properties of fish hemoglobins: kinetics of reaction with oxygen and carbonmonoxide of the isolated hemoglobin components from trout (*Salmo irideus*). *Eur. J. Biochem.* 39:571–579.

Herzfeld, J., and E. Stanley. 1974. A general approach to cooperativity and its application to the oxygen equilibrium of hemoglobin and its effectors. *J. Mol. Biol.* 82:231-265.

Hoard, J. L. 1971. Stereochemistry of hemes and other metalloporphyrins. *Science* (*Wash. DC*). 174:1295–1302.

Hopfield, J. J. 1973. Relation between structure, cooperativity and its application to the oxygen equilibrium of hemoglobin action. *J. Mol. Biol.* 104:707–722.

Hsu, M. C. 1970. Optical activity of heme proteins, PhD-thesis. Urbana, Illinois.

Kwiatkowski, L., and R. W. Noble. 1982. The contribution of histidine(HC3)(146β) to the R-state Bohr effect of human hemoglobin. *J. Biol. Chem.* 257:8891-8895.

Kilmartin, J. V., J. H. Fogg, and M. F. Perutz. 1980. Role of the C-terminal histidine in the alkaline Bohr effect of human hemoglobin. *Biochemistry.* 19:3189–3193.

Loudon, R. 1973. The Quantum Theory of Light. Clarendon Press, Oxford.

Moffat, J. K. 1971. Structure and functional properties of chemically modified horse hemoglobin. *J. Mol. Biol.* 58:79–88.

Nagai, K., T. Kitagawa, and H. Morimoto. 1980. Quarternary stuctures and low frequency molecular vibrations of hemes of deoxy and oxyhaemoglobin studied by resonance Raman scattering. *J. Mol. Biol.* 136:271–289.

el Naggar, S., W. Dreybrodt, and R. Schweitzer-Stenner. 1985. Haem-Apoprotein interactions detected by resonance Raman scattering in Mb- and Hb-derivatives lacking the saltbridge His 146β-Asp 94β. *Eur. Biophys. J.* 12:43–49.

Ondrias, M. R., D. L. Rousseau, J. A. Shelnutt, and S. R. Simon. 1982. Quarternary-transformation induced changes at the heme in deoxyhemoglobin. *Biochemistry.* 31:3420–3427.

Perutz, M. F. 1970*a*. Stereochemistry of cooperative effects in haemoglobin. *Nature* (*Lond.*). 228:726–734.

Perutz, M. F. 1970*b*. The Bohr effect and combinations with organic phosphates. *Nature* (*Lond.*). 228:734–739.

Perutz, M. F., and M. Brunori. 1982. Stereochemistry of cooperative effects in fish and amphibian haemoglobin. *Nature* (*Lond.*). 299:421–426.

Perutz, M. F., G. Fermi, and T. B. Shih. 1984. Structure of deoxyhemoglobin cowtown HisHC3(146)$\beta \rightarrow$ Leu: origin of the alkaline Bohr effect and electrostatic interactions in hemoglobin. *Proc. Natl. Acad. Sci. USA.* 81:4781–4784.

Perutz, M. F., A. M. Gronenborn, G. M. Clore, J. H. Fogg, and T. B. Shih. 1985. The pK_a-value of two histidine residues in human haemoglobin, the Bohr effect and the dipolement of the α-helix. *J. Mol. Biol.* 183:491-498.

Peticolas, W., L. Nafie, P. Stein, and B. Fanconi. 1970. Quantum theroy of the intensities of molecular vibrational spectra. *J. Chem. Phys.* 52:1576-1588.

Russu I., N. T. Ho, and C. Ho. 1982. A proton nuclear magnetic resonance investigation of histidyl residues in human adult hemoglobin. *Biochemistry.* 21:5031–5034.

Rousseau, D., S. L. Tan, M. R. Ondrias, S. Ogawa, and R. W. Noble. 1984. Absence of cooperativity energy at the heme in ligand hemoglobin. *Biochemistry.* 23:2857–2865.

Schweitzer-Stenner, R., D. Wedekind, W. Dreybrodt, and S. el Naggar. 1984. Investigation of pH-induced symmetry distortions of the prosthetic group in oxyhaemoglobin by resonance Raman scattering. *Eur. Biophys. J.* 11:61–67.

Schweitzer-Stenner, R., and W. Dreybrodt. 1985. Excitation profiles and depolarisation ratios of some prominent Raman lines in oxyhaemoglobin and ferrocytochrome c in the preresonant and resonant region of the Q-band. *J. Raman Spectrosc.* 16:111–132.

Schweitzer-Stenner, R., D. Wederkind, and W. Dreybrodt. 1986. Correspondence of the pK-values of oxyHb-titration states detected by resonance Raman scattering to kinetic data of ligand dissociation and association. *Biophys. J.* 49:1077–1088.

Schweitzer-Stenner, R., and W. Dreybrodt. 1988. An extended MWC-model expressed in terms of the Herzfeld-Stanley formalism applied to oxygen and carbonmonoxide binding curves of hemoglobin trout IV. *Biophys. J.* 55:691–701.

Shaanan, B. 1983. Structure of human oxyhemoglobin at 2:1 Å resolution. *J. Mol. Biol.* 171:31–59.

Shelnutt, J. A., D. L. Rousseau, J. M. Friedman, and S. R. Simon. 1979. Protein interaction in hemoglobin: evidence from Raman difference spectroscopy. *Proc. Natl. Acad. Sci. USA.* 76:4409–4413.

Warshel, A. 1977. Energy-structure correlation in metalloporphyrins and the control of oxygen binding by hemoglobin. *Proc. Natl. Acad. Sci. USA.* 74:1789–1793.

Wedekind, D., R. Schweitzer-Stenner, and W. Dreybrodt. 1985. Heme-apoprotein interaction in the modified oxyhemoglobin-bis-(*N*-maleimidomethyl) ether and in oxyhemoglobin at high Cl^--concentration detected by resonance Raman scattering. *Biochim. Biophys. Acta.* 830:224–232.

Wedekind, D., U. Brunzel, R. Schweitzer-Stenner, and W. Dreybrodt. 1986. Correlation of pH-dependent resonance Raman and optical absorption data reflecting heme-apoprotein interaction in oxyhaemoglobin. *J. Mol. Struct.* 143:457–460.